Inorganica Chimica Acta, 150 (1988) 177–181

Crystal and Molecular Structure of μ-Oxo-bis((5,10,15,20)tetrakispentafluorophenyl)-porphinatoiron(III)

A. GOLD*, K. JAYARAJ

University of North Carolina at Chapel Hill, Chapel Hill, N.C. 27514, U.S.A.

P. DOPPELT, J. FISCHER and R. WEISS*

Université Louis Pasteur, Institut le Bel, Strasbourg Cédex 67070, France

(Received December 21, 1987)

Abstract

In this paper, we report the crystal and molecular structure of μ-oxo-bis(5,10,15,20)tetrakispentafluorophenyl)porphinatoiron(III) [(TPP(F$_5$)Fe)$_2$O]. The crystals belong to the tetragonal system, space group $I4_1/a$, with $a = b = 26.362(7)$, $c = 30.886(8)$ Å, $V = 21465$ Å^3, $Z = 8$ and $D_{\text{calc}} = 1.496$. Discrepancy indices are $R_1 = 0.084$ and $R_2 = 0.104$ for 3320 reflections having $I > 3\sigma(I)$. The Fe–N$_p$ average distance, 2.088(11) Å, is at the long end of the range of high-spin ferric porphyrin while the Fe–O distances (1.775(1) Å) are similar to those of the non-halogenated analog (TPPFe)$_2$O. The Fe–O–Fe angle of 178.4(5)° shows an essentially linear oxo bridge. The 0.673(2) Å displacement of the iron atom from the porphyrin mean plane is unusually large. The facing porphyrin rings are twisted 47° with respect of each other giving the molecule nearly exact D_{4d} symmetry.

Introduction

The generation of observable high-valent iron monooxygen species from tetramesitylporphinatoiron complexes has evoked considerable interest in the bifacially hindered complexes as models for biological monooxygen transfer catalysis [1–10] and a number of such compounds have been synthesized for this purpose [1, 5, 7, 10]. The highly halogenated complexes, *meso* 2,6-dichlorophenyl [5] and *meso* pentafluorophenylporphinatoiron(III) [1] have proven to be effective catalysts, highly resistant to oxidative degradation. To date, studies on the mechanisms of monooxygen transfer by these compounds have not been complemented by any molecular structure determinations, leaving a gap in knowledge necessary for complete understanding of the formation and reactivity of the catalytically competent intermediates. We report here the crystal and molecular structure of μ-oxo-bis((5,10,15,20)tetrakispentafluorophenyl)porphinatoiron(III) [(TPP(F$_5$)Fe)$_2$O] (Fig. 1). This compound is of interest not only as a halogenated porphyrin, but also because the *o*-fluorine atoms of the *meso*-phenyl groups appear to offer only marginal encumberance of the iron, permitting the existence of a hydroxo complex under certain conditions [11]. In addition, the μ-oxo-bridged compound exhibits significantly increased antiferromagnetic coupling between the iron centers in the solid state compared to in solution [12].

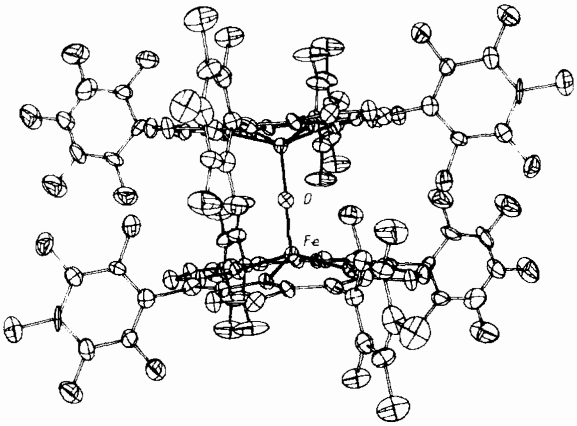

Fig. 1. ORTEP plot of (TPP(F$_5$)Fe)$_2$O. Ellipsoids are scaled to enclose 50% of the electron density. Hydrogen atoms are omitted.

Experimental

The μ-oxo bridged complex was synthesized and purified by published methods [12]. The red crystals obtained by evaporation of a heptane solution were only marginally suitable for X-ray diffraction. The crystals degraded rapidly on removal from the mother liquor and all manipulations were performed under cold conditions (−20 °C).

---

*Authors to whom correspondence should be addressed.

0020-1693/88/$3.50

© Elsevier Sequoia/Printed in Switzerland

The diffraction data were collected at −100 °C on a Philips PW1100/16 diffractometer using Cu Kα graphite monochromated radiation ($\lambda = 1.5405$ Å). A parallepiped-shaped crystal was cut from a cluster and glued to a glass filament mounted on a rotation free goniometer head. Data collection parameters are given in Table I. The orientation matrix was obtained from 25 machine-centered reflections. Three standard reflections measured every hour showed no trend in intensity during data collection. No equivalent reflections were recorded. The raw step scan data were converted to intensities using the Lehmann–Larsen [13a] method and then corrected for Lorentz, polarization and absorption factors, the latter computed by the empirical method of Walker and Stuart [13b] since face indexing was not possible. The structure was solved by Patterson techniques. After refinement of the heavy atoms, difference Fourier maps revealed maxima of electron density close to the positions expected for hydrogen atoms. Hydrogen atoms were introduced into the structure factor calculation by their computed coordinates (C–H = 0.95 Å) and isotropic temperature factors such that $B(\mathrm{H}) = 1 + B_{\mathrm{eq}}(\mathrm{C})$ Å^2. No hydrogen atom parameter was allowed to vary during full-matrix least-squares refinement minimizing $\Sigma w(|F_o| - |F_c|)^2$. The unit-weight observation in Table I is for $p = 0.08$ in $\sigma^2(F^2) = \sigma^2_{\mathrm{counts}} + (pI)^2$. A final difference map showed no significant maxima. The scattering factors and anomalous dispersion coefficients were taken from refs. 14 and 15 respectively. For all computations, the Enraf-Nonius SPD/VAX package was used [16]. See also 'Supplementary Material'.

TABLE I. Crystallographic Data

Formula	$C_{112}H_{72}NOF_{40}Fe_2$
Molecular weight	2417.51
Crystal system	tetragonal
$a = b$ (Å)	26.362(7)
c (Å)	30.886(8)
V (Å^3)	21465
Z	8
D_{calc}	1.496
μ(cm^{-1})	32.678
Crystal dimension (mm)	0.30 × 0.30 × 0.40
Space group	$I4_1/a$
Scan mode	flying step-scan
Scan angle	1.0 + 0.143 tan(θ)
Scan speed (° mn^{-1})	0.024
Octant	$+h$ $+k$ $+l$
Theta range (°)	3/57
No. data measured	7605
No. data with $I > 3\sigma(I)$	3320
Abs. min./max.	0.43/2.5
R_1	0.084
R_2	0.104
GOF	1.82

Discussion

The compound crystallized in space group $I4_1/a$ with 2 μ-oxo molecules and 8 solvent molecules in the unit cell. The included solvent was hexane, apparently present in heptane as a minor impurity. Positional parameters are given in Table II, selected bond lengths and angles in Table III. An ORTEP plot is shown in Fig. 1. As expected for high-spin ferric porphyrins, the coordination spheres of the iron atoms are square pyramidal [17, 18]. Close adherence of the complex to four-fold symmetry is evident in the small estimated standard deviations of the averaged core parameters (Table III). The metal–pyrrole nitrogen distance (Fe–N_p) of 2.088(11) Å is at the long end of the range of high-spin ferric porphyrins, while the 2.015(5) Å distance between N_p and the center of the plane defined by the pyrrole nitrogens (C_t) reflects maintenance of optimum core size [17]. The Fe–O distances of 1.775(1) Å are similar to those of the μ-oxo bridged complex of tetraphenylporphinatoiron(III) ((TPP)-Fe)$_2$O) and the Fe–O–Fe angle of 178.4(5)° shows an essentially linear oxo bridge in contrast to the small but significant 3° bending of ((TPP)Fe)$_2$O [19, 20]. The 0.673(2) Å displacement of the iron atoms of (TPP(F$_5$)Fe)$_2$O from the porphyrin mean plane is unusually large.

Bond lengths and angles of the porphyrin ligands are almost identical to those of the TPP complex, indicating no strain or distortion of the porphyrin skeletons; however pronounced doming is evident in the uniform tilting of the planes of the pyrrole rings away from iron, which results in a 0.13 Å difference between the mean planes of the pyrrole nitrogen atoms and the porphyrin cores (Fig. 2).

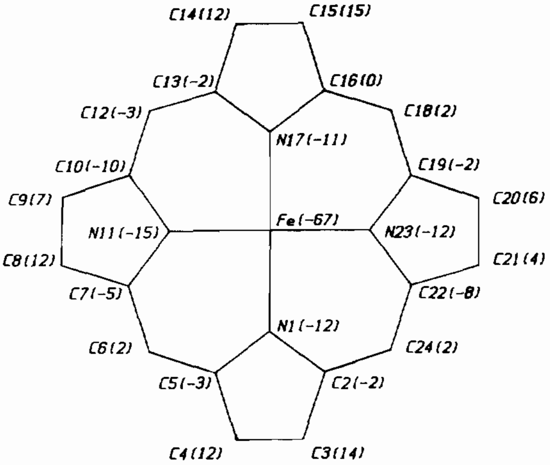

Fig. 2. Stick model for the porphyrin core present in (TPP-(F$_5$)Fe)$_2$O. Numbers indicate in 0.01 Å the deviations from the 24-atoms core mean plane.

TABLE II. Table of Positional Parameters[a]

Atom	*x*	*y*	*z*	*B* (Å^2)[b]
Fe	0.01669(7)	−0.18477(7)	0.12076(6)	2.47(4)
O	0.000	−0.250	0.1215(4)	3.2(3)
N1	−0.0108(3)	−0.1562(4)	0.0623(3)	2.6(2)
C2	0.0120(5)	−0.1593(5)	0.0213(4)	3.1(3)
C3	−0.0247(5)	−0.1426(5)	−0.0106(4)	3.5(3)
C4	−0.0678(5)	−0.1310(5)	0.0096(5)	3.9(3)
C5	−0.0579(5)	−0.1391(5)	0.0549(4)	2.5(3)
C6	−0.0946(5)	−0.1257(5)	0.0864(4)	3.4(3)
C7	−0.0884(4)	−0.1297(4)	0.1307(4)	2.5(3)
C8	−0.1224(5)	−0.1124(5)	0.1631(4)	3.3(3)
C9	−0.1007(4)	−0.1201(5)	0.2024(4)	3.3(3)
C10	−0.0517(5)	−0.1411(5)	0.1948(4)	3.1(3)
N11	−0.0434(4)	−0.1465(4)	0.1499(3)	2.9(2)
C12	−0.0146(5)	−0.1489(5)	0.2249(4)	2.8(3)
C13	0.0355(4)	−0.1630(5)	0.2181(4)	2.4(3)
C14	0.0734(5)	−0.1677(5)	0.2515(4)	3.1(3)
C15	0.1182(5)	−0.1798(5)	0.2305(4)	3.2(3)
C16	0.1070(4)	−0.1834(4)	0.1865(4)	2.7(3)
N17	0.0564(4)	−0.1730(4)	0.1781(3)	2.6(2)
C18	0.1429(5)	−0.1933(5)	0.1547(4)	3.1(3)
C19	0.1337(4)	−0.1932(5)	0.1112(4)	3.2(3)
C20	0.1727(5)	−0.2018(5)	0.0785(5)	3.9(3)
C21	0.1495(5)	−0.1963(6)	0.0390(4)	4.0(3)
C22	0.0966(5)	−0.1860(5)	0.0466(4)	3.0(3)
N23	0.0884(4)	−0.1843(4)	0.0908(3)	3.2(2)
C24	0.0614(5)	−0.1721(5)	0.0146(4)	3.0(3)
C25	−0.1450(5)	−0.1028(5)	0.0711(4)	3.1(3)
C26	−0.1888(5)	−0.1296(5)	0.0665(5)	4.9(4)
C27	−0.2315(5)	−0.1069(6)	0.0525(5)	5.0(4)
C28	−0.2336(5)	−0.0605(6)	0.0408(5)	4.9(4)
C29	−0.1928(6)	−0.0324(6)	0.0440(6)	6.7(5)
C30	−0.1472(5)	−0.0534(5)	0.0597(6)	4.9(4)
F1	−0.1887(3)	−0.1791(3)	0.0790(4)	8.8(3)
F2	−0.2745(3)	−0.1355(4)	0.0506(4)	11.0(4)
F3	−0.2767(3)	−0.0393(4)	0.0267(4)	8.2(3)
F4	−0.1919(4)	0.0171(4)	0.0327(5)	11.4(4)
F5	−0.1045(3)	−0.0247(3)	0.0609(4)	8.8(3)
C31	−0.0289(5)	−0.1394(5)	0.2733(4)	2.8(3)
C32	−0.0219(5)	−0.0933(5)	0.2922(4)	3.3(3)
C33	−0.0328(5)	−0.0848(5)	0.3348(4)	3.4(3)
C34	−0.0532(5)	−0.1224(6)	0.3577(4)	4.0(3)
C35	−0.0612(5)	−0.1694(5)	0.3402(5)	3.7(3)
C36	−0.0492(5)	−0.1769(5)	0.2972(4)	3.0(3)
F6	−0.0012(3)	−0.0549(3)	0.2684(3)	4.9(2)
F7	−0.0234(4)	−0.0385(3)	0.3521(3)	5.6(2)
F8	−0.0637(3)	−0.1142(3)	0.4001(3)	5.7(2)
F9	−0.0801(3)	−0.2063(3)	0.3653(3)	6.1(2)
F10	−0.0553(3)	−0.2242(3)	0.2816(3)	4.5(2)
C37	0.1962(5)	−0.2015(5)	0.1703(4)	3.3(3)
C38	0.2301(5)	−0.1643(5)	0.1725(5)	4.0(3)
C39	0.2780(5)	−0.1718(5)	0.1869(5)	4.1(3)
C40	0.2929(4)	−0.2192(5)	0.1998(4)	3.4(3)
C41	0.2598(5)	−0.2576(5)	0.1974(4)	3.2(3)
C42	0.2126(5)	−0.2480(5)	0.1829(4)	3.2(3)
F11	0.2166(3)	−0.1168(3)	0.1614(3)	6.9(3)
F12	0.3119(3)	−0.1326(3)	0.1906(4)	7.8(3)
F13	0.3402(3)	−0.2264(3)	0.2151(3)	5.5(2)
F14	0.2747(3)	−0.3043(3)	0.2102(3)	4.7(2)

(continued)

TABLE II. *(continued)*

Atom	*x*	*y*	*z*	B (Å^2)^b
F15	0.1801(3)	−0.2881(3)	0.1809(3)	4.6(2)
C43	0.0812(5)	−0.1707(5)	−0.0307(4)	2.7(3)
C44	0.0790(6)	−0.2105(5)	−0.0583(4)	4.1(3)
C45	0.0978(6)	−0.2064(6)	−0.1011(5)	5.2(4)
C46	0.1170(5)	−0.1622(6)	−0.1147(4)	4.3(4)
C47	0.1201(6)	−0.1229(6)	−0.0876(5)	5.2(4)
C48	0.1026(6)	−0.1264(6)	−0.0462(4)	4.9(4)
F16	0.0597(4)	−0.2543(3)	−0.0459(3)	7.8(3)
F17	0.0947(4)	−0.2466(3)	−0.1269(3)	8.2(3)
F18	0.1352(3)	−0.1590(3)	−0.1559(2)	6.0(2)
F19	0.1395(4)	−0.0787(4)	−0.1018(3)	9.4(3)
F20	0.1039(5)	−0.0862(3)	−0.0200(3)	9.1(3)
CS1	0.235(2)	−0.002(2)	0.838(2)	13(2)*
CS2	0.260(2)	0.035(2)	0.837(2)	10(1)*
CS3	0.307(2)	0.058(3)	0.833(2)	17(2)*
CS4	0.341(2)	0.045(2)	0.795(2)	15(2)*
CS5	0.372(2)	0.030(2)	0.757(2)	11(1)*
CS6	0.373(2)	0.020(2)	0.713(2)	14(2)*
CS7	0.928(1)	0.041(1)	0.204(1)	6.9(9)*
CS8	0.958(2)	0.036(2)	0.178(1)	9(1)*
CS9	0.983(1)	0.003(1)	0.160(1)	8(1)*
CS10	1.016(2)	−0.001(2)	0.132(2)	11(1)*
CS11	1.043(2)	−0.022(2)	0.121(2)	14(2)*
CS12	1.080(2)	−0.036(3)	0.110(2)	17(2)*

[a] e.s.d.s given in parentheses. [b] Starred atoms were refined isotropically. Anisotropically refined atoms are given in the form of the isotropic equivalent displacement parameter defined as: $(4/3)[a^2\beta(1,1) + b^2\beta(2,2) + c^2\beta(3,3) + ab(\cos\gamma)\beta(1,2) + ac(\cos\beta)\beta(1,3) + bc(\cos\alpha)\beta(2,3)]$.

TABLE III. Selected Bond Lengths (Å) and Bond Angles (°)

Fe–N$_1$	2.085(7)	O–Fe–N$_1$	106.0(3)
Fe–N$_{11}$	2.082(7)	O–Fe–N$_{11}$	106.0(3)
Fe–N$_{17}$	2.081(6)	O–Fe–N$_{17}$	105.0(3)
Fe–N$_{23}$	2.104(7)	O–Fe–N$_{23}$	103.5(2)
Fe–Np	2.088(4)		
Fe–O	1.775(1)		
N–C$_\alpha$	1.384(3)	N–C$_\alpha$–C$_\beta$	110.0(2)
C$_\alpha$–C$_\beta$	1.434(4)	C$_\alpha$–N–C$_\alpha$	105.7(3)
C$_\beta$–C$_\beta$	1.361(6)	C$_\alpha$–C$_\beta$–C$_\beta$	107.1(3)
C$_\alpha$–C$_m$	1.384(4)	N–C$_\alpha$–C$_m$	124.8(3)
C$_m$–C$_{phe}$	1.523(6)	C$_{phe}$–C$_{phe}$–C$_{phe}$	120.0(3)
C–F	1.350(2)		
C$_{phe}$–C$_{phe}$	1.353(2)		

The facing porphyrin rings are twisted 47° with respect to each other, giving the molecule nearly exact D_{4d} symmetry (Fig. 3).

Although the steric requirements of the *o*-fluorine substituents of the *meso*-phenyl groups are not sufficiently stringent to prevent formation of the μ-oxo bridged system, effects of steric interactions are evident on comparison of this structure to that of ((TPP)Fe)$_2$O. The pronounced doming of (TPP(F$_5$)Fe)$_2$O and the large displacement of iron from the mean plane of the 24-atom porphyrin core presumably results from interactions of the *o*-fluorines of the phenyl substituents of the facing porphyrins. This geometry contrasts with the slightly ruffled porphyrin rings of ((TPP)Fe)$_2$O and the 0.5 Å displacement of iron above the mean porphyrin plane, which is nearly coincident with the plane defined by the pyrrole nitrogens. While the dihedral angles between the planes of the phenyl rings of ((TPP)Fe)$_2$O and the mean plane of the core vary [19] from 8° to 37°, interactions between *o*-fluorines and pyrrole β-hydrogens cause the phenyl planes of (TPP(F$_5$)Fe)$_2$O to be virtually perpendicular to the mean porphyrin plane, with dihedral angles ranging from 1.3° to 8.8°. As a consequence, the facing porphyrin rings of (TPP(F$_5$)Fe)$_2$O are rotated with respect to each other so that phenyl groups are almost perfectly staggered, while the phenyls of ((TPP)Fe)$_2$O are somewhat closer to an eclipsed configuration [19] (Fig. 3).

Since the Fe–O distance is similar to that of ((TPP)Fe)$_2$O by virtue of doming and the long Fe–N$_p$ bonds, the similarity of the antiferromagnetic coupling in the solid state to that of the TPP μ-oxo complex is not surprising.

On both the inward Fe–O and outward faces of the pyrrole nitrogen mean plane, the *o*-fluorine atoms form cavities which may be defined by the

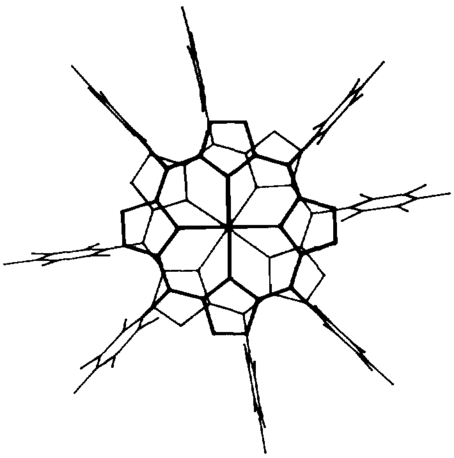

Fig. 3. Line–Stick projection of μ-oxo-bis((5,10,15,20)-tetrabispentafluorophenyl)porphinatoiron(III) along the Fe–O–Fe axis.

diagonal distances between *o*-fluorine atoms and by the mean distances of the *o*-fluorines from a plane through iron parallel to the pyrrole nitrogen mean plane. Cavity height on the inward Fe–O face can be estimated by subtraction of the Fe–C_t distance from the mean distance of the inward-facing *o*-fluorines below the pyrrole nitrogen mean plane and on the outside face by addition of the Fe–C_t distance to the mean distance of the outward-facing fluorines above the pyrrole nitrogen mean plane. As a result of the domed ligand, the cavities have distinctly different sizes. On the Fe–O face, the pocket height is 1.44 Å above the plane containing iron and the diagonal dimension is 10.60 Å. The pocket on the opposite face is 3.16 Å deep with a 9.34 Å diagonal. The large size of the $(TPP(F_5)Fe)_2O$ pockets is consistent with the low shape-selectivity observed in oxidations catalyzed by the bifacially hindered porphyrins (TMP)Fe(III) and $TPP(2,4,6\text{-}OCH_3)Fe(III)$ [9] and suggests that the importance of phenyl *o*-substituents in stabilizing putative monooxygen intermediates may be to protect the nucleophilic *meso* carbon atoms of the porphyrin core against oxidation. Further enlightenment regarding this conclusion awaits structural determination of additional complexes of bifacially hindered porphinatoirons.

Supplementary Material

Anisotropic temperature factors (Table S1); hydrogen atom parameters (Table S2); complete set of bond lengths (Table S3); complete set of bond angles (Table S4); and observed and calculated structure factor amplitudes for all observed reflections (X10) (Table S5) are available from the authors on request.

Acknowledgements

This work was supported in part by USPHS Grant £0ES03433. A.G. is the recipient of an NIH Senior International Fellowship.

References

1 C. K. Chang and F. Ebina, *J. Chem. Soc., Chem. Commun.*, 779 (1985).
2 J. T. Groves, R. C. Haushalter, M. Nakamura, T. E. Nemo and B. J. Evans, *J. Am. Chem. Soc.*, *103*, 2884 (1981).
3 D. Mansuy, J. F. Bartoli and M. Momenteau, *Tetrahedron Lett.*, *23*, 2781 (1982).
4 J. R. L. Smith and P. R. Sleath, *J. Chem. Soc., Perkin Trans. II*, 1009 (1982).
5 P. S. Traylor, D. Dolphin and T. G. Traylor, *J. Chem. Soc., Chem. Commun.*, 279 (1984).
6 J. P. Collman, T. Kodadek, S. A. Raybuck, J. I. Brauman and L. M. Papazain, *J. Am. Chem. Soc.*, *107*, 4343 (1985).
7 T. G. Traylor, J. C. Marsters, T. Nakano and B. E. Dunlap, *J. Am. Chem. Soc.*, *107*, 5537 (1985).
8 J. T. Groves and T. Watanabe, *J. Am. Chem. Soc.*, *108*, 507 (1986).
9 B. R. Cook, T. J. Reinert and K. S. Suslick, *J. Am. Chem. Soc.*, *108*, 7281 (1986).
10 T. G. Traylor and S. Tsuchiya, *Inorg. Chem.*, *26*, 1338 (1987).
11 K. Kayaraj, A. Gold, G. E. Toney, J. H. Helms and W. E. Hatfield, *Inorg. Chem.*, *25*, 3516 (1986).
12 J. H. Helms, L. W. TerHaarn, W. E. Hatfield, D. L. Harris, K. Jayaraj, G. E. Toney, A. Gold, T. D. Mewborn and J. E. Remberton, *Inorg. Chem.*, *25*, 2334 (1986).
13 (a) M. S. Lehmann and F. K. Larsen, *Acta Crystallogr., Sect. A*, *30*, 580 (1974); (b) N. Walker and D. Stuart, *Acta Crystallogr., Sect. A*, *39*, 158 (1983).
14 D. T. Cromer and J. T. Waber, 'International Tables for X-Ray Crystallography', Vol. IV, Kynoch Press, Birmingham, U.K., 1974, Table 2.2b.
15 D. T. Cromer, 'International Tables for X-Ray Crystallography', Vol. IV, Kynoch Press, Birmingham, U.K., 1974, Table 2.3.1.
16 B. A. Frenz, in H. Schenk, R. Olthof-Hazekamp, H. Van Koningsveld and C. G. Bassi (eds.), 'Computing in Crystallography', Delft University Press, Delft, The Netherlands, 1978, p. 64.
17 W. R. Scheidt and C. A. Reed, *Chem. Rev.*, *81*, 543 (1981).
18 W. R. Scheidt and M. P. Gouterman, in A. B. P. Lever and H. B. Gray (eds.), 'Iron Porphyrins', Part 1, Addison Wesley, New York, 1983, pp. 89–140.
19 A. B. Hoffmann, D. M. Collins, V. W. Day, E. B. Flesher, T. S. Srivastava and J. L. Hoard, *J. Am. Chem. Soc.*, *94*, 3620 (1972).
20 P. N. Swepston and J. A. Ibers, *Acta Crystallogr., Sect. C*, *41*, 671 (1985).